Biosensors and Bioelectronics 77 (2016) 733–739

Contents lists available at ScienceDirect

Biosensors and Bioelectronics

journal homepage: www.elsevier.com/locate/bios

Ratiometric electrochemiluminescent strategy regulated by electrocatalysis of palladium nanocluster for immunosensing

Yin Huang, Jianping Lei*, Yan Cheng, Huangxian Ju

State Key Laboratory of Analytical Chemistry for Life Science, Collaborative Innovation Center of Chemistry for Life Science, School of Chemistry and Chemical Engineering, Nanjing University, Nanjing 210093, PR China

ARTICLE INFO

Article history:
Received 24 June 2015
Received in revised form
25 September 2015
Accepted 12 October 2015
Available online 22 October 2015

Keywords:
Ratiometric electrochemiluminescence
Immunosensor
Quantum dots
Palladium nanocluster
Electrocatalysis

ABSTRACT

This work designed a novel ratiometric electrochemiluminescence (ECL) immunosensing approach based on two different ECL emitters: CdS quantum dots (QDs) as cathodic emitter and luminol as anodic emitter. The ECL immunosensor was constructed by a layer-by-layer modification of CdS QDs, Au nanoparticles and capture antibody on a glassy carbon electrode. With hydrogen peroxide as ECL coreactant, the immunosensor showed a cathodic ECL emission of CdS QDs at −1.5 V (vs Ag/AgCl) in air-saturated pH 8.0 buffer. Upon the formation of sandwich immunoassay, the lumiol/palladium nanoclusters (Pd NCs)@graphene oxide probe was introduced to the electrode. Therefore, the cathodic ECL intensity decreased and luminol anodic ECL emission was appeared at +0.3 V (vs Ag/AgCl) owing to the competition of the coreactant of hydrogen peroxide. Using carcino-embryonic antigen as model, this ratiometric ECL strategy could be used for immunoassay with a linear range of 1.0–100 pg mL^{-1} and a detection limit of 0.62 pg mL^{-1}. The enhanced ratiometric ECL signal resulted from the high density and excellent electrocatalysis of the loaded Pd NCs. The immunosensor exhibited good stability and acceptable fabrication reproducibility and accuracy, showing a great promising for clinical application. This electrocatalysis-regulated ratiometric ECL provides a new concept for ECL measurement, and could be conveniently extended for detection of other protein biomarkers.

1. Introduction

Electrogenerated chemiluminescence (ECL) is a new technique of producing light on an electrode surface by applying a potential (Deng and Ju, 2013; Shin et al., 2010), and exhibits remarkable sensitivity and versatile detection application due to the separation between the potential as excited signal and the light as detection signal. ECL technology has been extensively used in anion sensing (Cheng et al., 2014), sequence-specific DNA detection (Cao et al., 2006; Dennany et al., 2003; Zhang et al., 2013), cell recognition (Han et al., 2014; Li et al., 2011; Liu et al., 2003) and multiplex immunoassays (Lin et al., 2011; Liu et al., 2010; Yoon et al., 2003). A practical "off–on" or "on–off" sensing strategy was commonly used in ECL biosensors via a luminescent response to the binding of the analyte (Deng et al., 2014; Doeven et al., 2013; Zhao et al., 2015). However, in most of these strategies, the ECL signal depended on the environmental changes, such as the concentration of coreactant, the probe concentration, instrument and buffer conditions, could introduce a false positive or a negative error during the detection of trace level analyte. Inspired by ratiometric fluorescent strategy, a potential-dependent ECL ratiometric strategy was reasonable to make the detection more anti-interference in complex samples.

The detection principle of conventional ratiometric fluorescent strategy can be related to two types of processes: one is based on the structural change of one fluorescent substance by introducing the target analyte, leading to the different wavelength emissions (Ding and Tian, 2014; He et al., 2015; Yan et al., 2015). The other is utilized two different fluorescent substances along with fluorescence resonance energy transfer (FRET) to adjust their intensities by introducing the target analyte (Hu et al., 2013; Noor and Krull, 2014). As a variation of ratiometric fluorescence, several ratiometric ECL assays have been proposed in biological analysis with one variable structure ECL probe (Sun et al., 2015) or two FRET ECL probes (Cheng et al., 2014; Zhang et al., 2013). For example, a ratiometric ECL strategy was achieved by using the bimetallic Ru–Os complex at different wavelengths around 620 nm and 730 nm (Sun et al., 2015). A dual-potential ratiometric ECL sensing approach is designed for the detection of Mg^{2+} via electrochemiluminescence resonance energy transfer (ERET) between

* Corresponding author. Fax: +86 25 83593593.
E-mail address: jpl@nju.edu.cn (J. Lei).

http://dx.doi.org/10.1016/j.bios.2015.10.038
0956-5663/

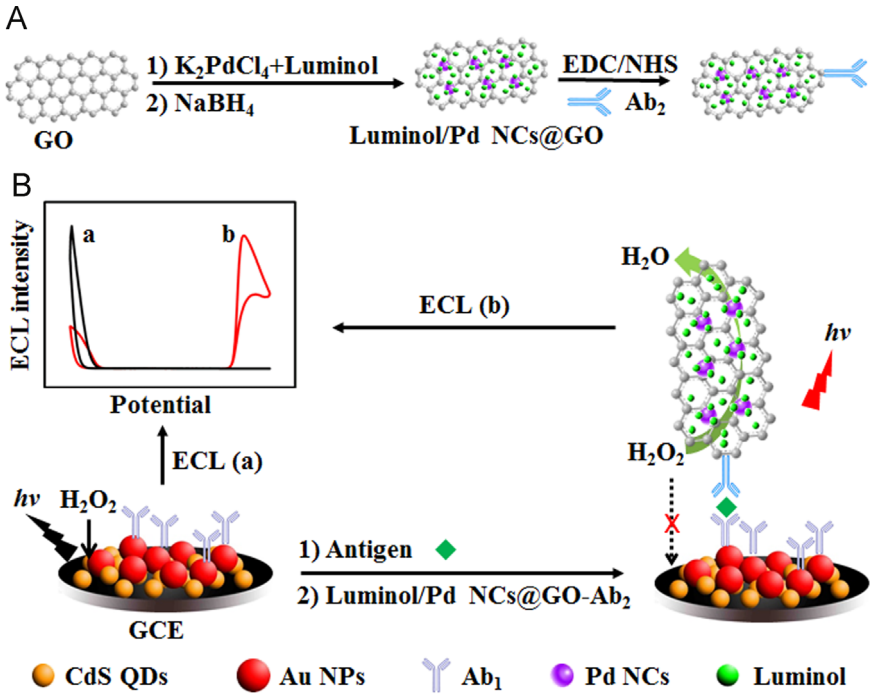

Scheme 1. Schematic illustration of (A) the synthesis of lumiol/Pd NCs@GO-Ab_2 probe, (B) ratiometric ECL approach regulated by electrocatalysis of Pd NCs for highly sensitive detection of CEA.

CdS quantum dots (QDs) and Cy5 molecule (Cheng et al., 2014). Xu and coworkers developed a dual enhancement ECL approach to detect telomerase activity from cancer cells (Zhang et al., 2014). Furthermore, unlike fluorescence, ECL has a high specificity due to the relationship between emitter and coreactant (Deng and Ju, 2013). Here, on the basis of the high catalytic ability of palladium nanoclusters (Pd NCs) toward hydrogen peroxide as coreactant (Nagaiah et al., 2013), we proposed a novel coreactant-dependent ratiometric ECL method with luminol and CdS QDs as ECL emitters.

The luminol-hydrogen peroxide system is well-known to produce a strong anode ECL emission at a variety of experimental condition (Cui et al., 2003, 2007). Recently, the luminol-functionalized noble metal nanoparticles probe has been employed in biosensor due to its catalytic property to accelerate electrochemical reaction associated with the luminol ECL process (He and Cui, 2012; Xu et al., 2011). In this work, luminol and CdS QDs as two different ECL emitters were integrated in one system for dual-potential ECL measurement of carcino-embryonic antigen (CEA) (Scheme 1). The ECL immunosensor was constructed by layer-by-layer immobilizing CdS QDs and Au nanoparticles (NPs) on an electrode, and then capture antibody (Ab_1) was connected to Au NPs via Au–S bond. With a sandwich immunoassay, the second antibody (Ab_2) modified luminol/Pd NCs@graphene oxide probe was captured on the immunosensor surface to competitively consume hydrogen peroxide as the coreactant for both luminol and CdS, leading to a decrease of cathode ECL emission intensity of CdS QDs at −1.5 V (Ag/AgCl) and an anodic ECL emission peak at +0.3 V (Ag/AgCl) from luminol. The proposed ratiometric immunoassay could detect protein with a detection limit down to picograms/milliliter level due to high density and excellent electrocatalysis of the loaded Pd NCs. Moreover, this method avoided the need of de-oxygenation for electrochemical immunoassay and thus provided a promising potential in clinical diagnosis, especially in point-of-care testing.

2. Materials and methods

2.1. Materials and reagents

Cadmium chloride ($CdCl_2 \cdot 2.5H_2O$) and thioglycolic acid (TGA) were purchased from Alfa Aesar China Ltd. $Na_2S \cdot 9H_2O$ was obtained from Shanghai Lingfeng Chemical Reagent Co. Ltd. Chloroauric acid ($HAuCl_4 \cdot 4H_2O$) was obtained from Shanghai Reagent Co. (Shanghai, China). Luminol, 1-ethyl-3-(3-(dimethylamino) propyl) carbodiimide (EDC), N-hydroxysuccinimide (NHS) and potassium tetrachloroplatinate (K_2PdCl_4) were purchased from Sigma-Aldrich. Both mouse monoclonal capture (Ab_1) and signal (Ab_2) anti-CEA antibodies (cloneno.27D6 and 28E4) were purchased from Shuangliu Zhenglong Biochem. Lab (Chengdu, China). CEA standard solutions were purchased from CEAELISA kit, which was supplied by Fujirebio Diagnostics AB (Göteborg, Sweden). Phosphate-buffered salines (PBS, 0.02 M) of various pHs were prepared by mixing the stock solutions of NaH_2PO_4 and Na_2HPO_4. The washing buffer was PBS (0.02 M, pH 7.4) containing 0.05% (w/v) Tween-20 (PBST). The clinical serum samples were from Jiangsu Institute of Cancer Prevention and Cure. Phosphate buffer solution (0.1 M, pH 8.0) containing 0.1 M KNO_3 was used throughout the ECL detection. Ultrapure water obtained from a Millipore water purification system ($\geq$ 18 MΩ, Milli-Q, Millipore) was used throughout the work. All other reagents were of analytical grade and used as received.

2.2. Apparatus

The ECL measurements were carried out on a MPI-E multifunctional electrochemical and chemiluminescent analytical system (Xi'an, China) at room temperature with the modified glassy carbon electrode (GCE, 5 mm in diameter, China) as working, a platinum wire as counter and a Ag/AgCl (saturated KCl) as reference electrodes. The emission window was placed in front of the photomultiplier tube biased at 1000 V. Photoluminescence

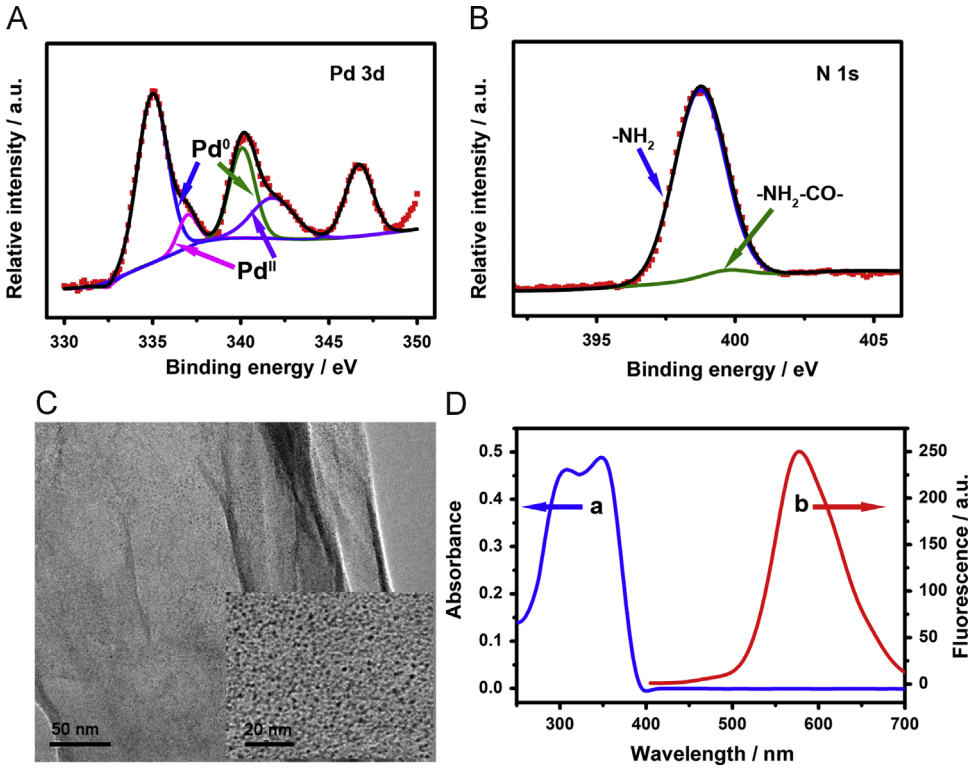

Fig. 1. XPS spectra for (A) Pd 3d, and (B) N 1s of the lumiol/Pd NCs@GO (the red dotted line is the measured spectrum; the black solid curve is the superposition of deconvoluted component spectrum). (C) TEM image of luminol/Pd NCs@GO, (D) UV–vis spectrum of luminol (a) and photoluminescence spectrum of CdS QDs (b).

(PL) spectra were obtained on a RF-5301 PC fluorometer (Shimadzu Co., Japan). UV – vis absorption spectra were obtained with a UV-3600 UV – vis – NIR spectrophotometer (Shimadzu Co., Kyoto, Japan). Transmission electron microscopic (TEM) images were obtained on JEM-2100 (Japan). X-ray photoelectron spectroscopy (XPS) measurements were performed using a PHI5000 Versa Probe spectrometer (ULVAC-PHI, Japan).

2.3. Preparation of QDs

CdS QDs were synthesized according to the previous report (Zhao et al., 2012). Typically, 250 μL of thioglycolic acid was injected into 50 mL of 0.01 M $CdCl_2$ (aq), and highly pure N_2 was bubbled for 30 min. After being adjusted to pH 11 with 1.0 M NaOH, 5.0 mL of 0.1 M Na_2S (aq) was injected. The resulting mixture solution was subsequently heated to 110 °C and refluxed for 4 h to obtain TGA-capped water-soluble CdS QDs. Finally, the as-prepared QDs solution was diluted with the same volume of water and kept in a refrigerator at 4 °C. Before usage, this QDs solution was sedimentated with isopropyl alcohol and collected by centrifugation. The colloidal precipitate was dissolved with an equivalent amount of deionized water for subsequent experiments.

2.4. Preparation of luminol/Pd NCs@GO-Ab_2 composite

All glassware used in the following procedures was cleaned in a bath of freshly prepared HNO_3/HCl (3:1, v/v), rinsed thoroughly in redistilled water, and dried prior to use. A 4 ml of 0.25 mg mL^{-1} GO aqueous solution was mixed with 200 μL of 1.0 mM K_2PdCl_4/luminol (1:1) and cooled to 0 °C with an ice bath. With stirring vigorously, 1.0 mg $NaBH_4$ was added rapidly. When the solution was maintained at 0 °C for 1 h, a color change from light yellow to light brown was observed. The solution was kept stirring vigorously until the solution turned into dark brown. The solution was centrifuged to remove the unreacted substance and the precipitate was further purified with ultrapure water 3 times. The precipitates were then resuspended in aqueous solution and stored at 4 °C.

Luminol/Pd NCs-GO was firstly activated in 0.01 M PBS buffer (pH 5.3) containing 10 mM EDC and 20 mM NHS for 1 h at room temperature. After this activated electrode was rinsed with PBS, 9 μL of 1.3 mg mL^{-1} anti-CEA antibody (Ab_2) was added to the solution, followed by incubating at 4 °C overnight. Afterwards, the excess of antibody was removed by centrifugation (12,000 rpm, 30 min at 4 °C) and redispersed in 10 mM PBS containing 0.1 M KCl. The obtained composite was redispersed in 2 mL of 0.01 M pH 7.4 PBS containing 0.1 M KCl and stored at 4 °C.

2.5. Preparation of ECL immunosensor

A GCE with 5 mm diameter was polished to a mirror using 1.0, 0.3, and 0.05 μm alumina slurry (Beuhler) followed by rinsing thoroughly with deionized water. After successive sonication in 1:1 nitric acid, acetone and deionized water, the electrode was rinsed with water and allowed to dry at room temperature. Then, 20 μL of 10 μM TGA–CdS QDs was dropped on the GCE and dried in air. Three microliter of 0.05% chitosan solution was coated on the film. After activating the chitosan film with 5 μL of Au colloidal solution at room temperature for 4 h, 5 μL of 0.1 mg mL^{-1} anti-CEA antibody (Ab_1) was coated on the electrode by an overnight incubation at 4 °C. Subsequently, the resulting electrode was washed three times with PBST and PBS to remove the physically absorbed Ab_1 and blocked with 10 μL of 5% BSA solution for 1 h at room temperature to obtain the ECL immunosensor.

3. Results and discussion

3.1. Characterization luminol/Pd NCs@GO

XPS was employed to analyze the chemical composition and status of the luminol/Pd NCs@GO (Fig. 1A). The binding energy of 335.0 eV (Pd $3d_{5/2}$) and 340.1 eV (Pd $3d_{3/2}$), which corresponds to the metallic Pd (0) state, demonstrates the presence of metallic Pd in as-prepared luminol/Pd NCs@GO. Meanwhile, the binding energy of 337.0 eV (Pd $3d_{5/2}$) and 341.8 eV (Pd $3d_{3/2}$) corresponds to the oxidation Pd species, which might be responsible for the incomplete reduction of the Pd species. Furthermore, through Gauss–Lorentzian curve fitting, we deconvoluted the *N* 1s spectrum of luminol/Pd NCs@GO with two peak at 398.8 eV and 399.7 eV (Fig. 1B), corresponding to the response of nitrogen atoms in the amine group (–NH_2) and amide group (–NH–CO–), respectively (Cui et al., 2007). TEM image was also employed to characterize the synthesis of luminol/Pd NCs@GO. As shown in Fig. 1C, the GO exhibited a few layered, which could provide three dimensional matrixes to enhance the loading of Pd NCs and facilitate electron transfer between Pd NCs and the adsorbed H_2O_2 (Zhang et al., 2005). Besides, Pd NCs were homogeneously decorated on the surface of GO with a diameter of ~1.0 nm (Fig. 1C, inset), leading to a high heterogeneous catalytic rate. Fig. 1D showed the UV–vis absorption spectrum of luminol (curve a) and fluorescence spectrum of CdS QDs (curve b) used in this experiment. The luminol exhibited two main UV–vis absorption peaks at 310 nm and 360 nm, which were attributed to aromatic amine groups. The CdS QDs has a sharp fluorescence emission at 592 nm resulted from the band-gap emission of the core (Jie et al., 2007). Obviously, there is no spectral overlap, indicating no FRET between luminol and CdS QDs.

3.2. Feasibility of the biosensor

ECL-potential responses were investigated at the stepwise steps to confirm the feasibility of the method in Fig. 2A. As control, the CdS QDs/Au NPs/Ab_1 modified GCE without CEA showed a cathodic ECL emission at −1.5 V (vs Ag/AgCl) in air-saturated 0.1 M pH 8.0 PBS buffer with 3.0 mM H_2O_2 (curve a). After incubation of CEA and the probe, the biosensor exhibited a significant 70.1% decrease in the cathode ECL intensity, and a new anode ECL peak of luminol appeared at around +0.30 V (curve c), resulting a potential-dependent ratiometric ECL approach. However, when using GO/luminol-Ab_2 as signal tracer (curve b), the cathode ECL intensity only decreased 32.7%, and the anodic ECL intensity increased 45.9% than that of using luminol/Pd NCs@GO-Ab_2 as the probe, indicating the Pd NCs on the GO greatly enhanced sensitivity of the biosensor.

In air-saturated pH 8.0 PBS buffer containing 0.1 M KNO_3 and 3.0 mM H_2O_2, the luminol/Pd NCs@GO modified electrode showed two cathodic peaks at −0.30 V and −0.9 V (Fig. 2B, curve a). After bubbling with N_2, luminol/Pd NCs@GO modified electrode still remains a peak current at −0.3 V with peak current of 25.3 μA (Fig. 2B, curve c), indicating the strong electrocatalytic reduction of luminol/Pd NCs@GO toward H_2O_2 as cathodic coreactant, leading to the decrease of cathodic ECL emission of CdS QDs. However, without Pd NCs, luminol@GO modified electrode showed a cathodic peak at −0.9 V with peak currents of 33.9 μA (Fig. 2B, curves b and d), which corresponds to the electrocatalytic reduction of luminol@GO toward O_2. Moreover, compared curve c with curve d, the oxidation peak of luminol starting from 0 V was significantly increased by introducing the Pd NCs to the surface of the electrode, implying that Pd NCs can enhance the anodic ECL emission of luminol.

3.3. Optimization of conditions for ECL detection

To achieve excellent performance in the ECL assay of CEA, several experiment parameters such as the pH of detection solution, the concentration of the coreactant H_2O_2, the incubation time and the amount of probe were optimized in Fig. 3. The ECL intensity increased with the increasing of the pH value of detection solution because the electrogenerated intermediates of H_2O_2 as the coreactant were more stable at high pH (Fig. 3A). Taking into account the bioactivity of immunoreagents, 0.1 M pH 8.0 PBS buffer was used through the following experiments. On the other hand, the dependence of ECL intensity on the concentration of H_2O_2 in the detection buffer was investigated in Fig. 3B. When 3.0 mM H_2O_2 was added, the ECL intensity reached the platform. With the further increasing of coreactant H_2O_2, ECL intensity was increased slightly due to the saturated radical on the surface of the

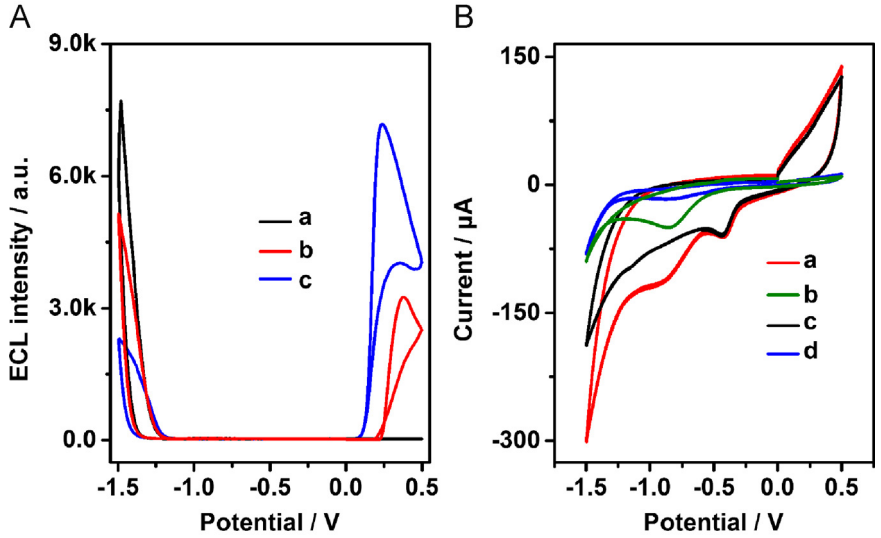

Fig. 2. (A) ECL spectra of CdS QDs/Au NPs/Ab_1 modified GCE in the absence of CEA with lumiol/Pd NCs@GO-Ab_2 (a), and presence of CEA with lumiol @GO-Ab_2 (b) and lumiol/Pd NCs@GO-Ab_2 (c) in air-saturated pH 8.0 PBS buffer containing 0.1 M KNO_3 and 3.0 mM H_2O_2. (B) CVs of luminol/Pd NCs@GO (a and c), luminol@GO (b and d) modified GCE in air- (a and b) and N_2– (c and d) saturated pH 8.0 PBS buffer containing 0.1 M KNO_3 and 3.0 mM H_2O_2.

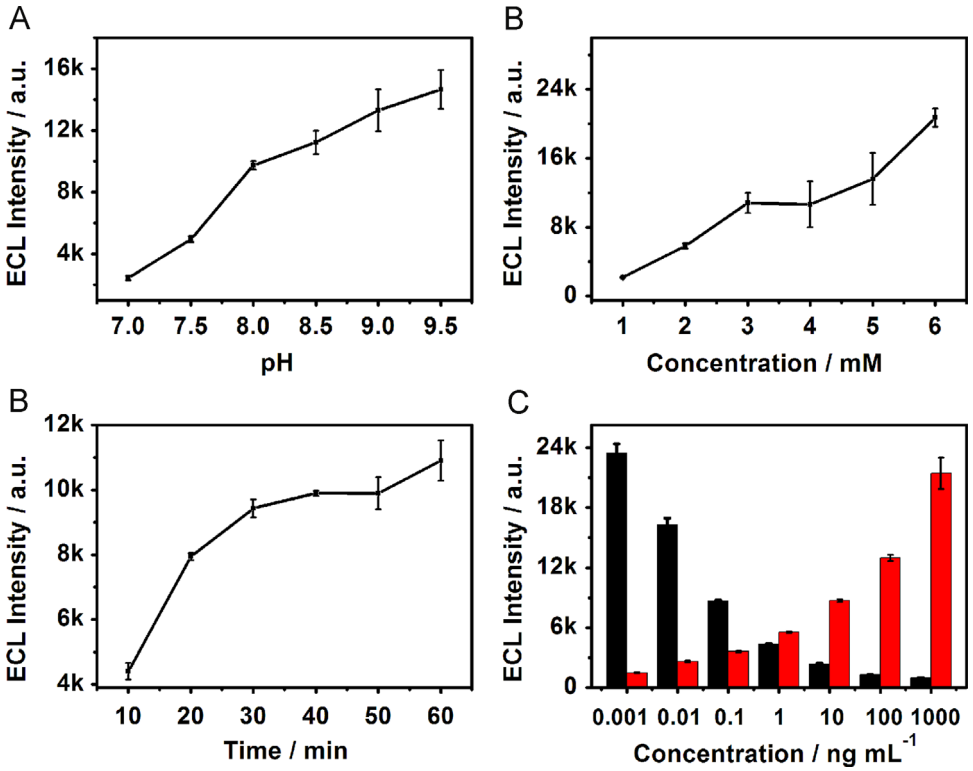

Fig. 3. Effects of (A) pH of detection solution, (B) concentration of H_2O_2 in the detection solution, (C) incubation time of lumiol/Pd NCs@GO-Ab_2 probe, and (D) concentration of lumiol/Pd NCs@GO-Ab_2 on ECL response of the immunosensor. When changing a parameter, the others are setting at their optimal conditions.

electrode. Therefore, 3.0 mM was favorable for this system as the optimal concentration.

Meanwhile, incubation time of immunization also affected the performance of this biosensor. As shown in Fig. 3C, the desirable ECL intensity change was obtained at 30 min in the presence of 10 pg mL^{-1} CEA. To efficiently facilitate ECL detection, 30 min was selected as the optimal reaction time. In addition, since luminol was employed as an ECL emitter, the concentration of the probe dramatically influenced the detection sensitivity of the proposed biosensor. As displayed in Fig. 3D, with an increasing concentration of probe, the ECL intensity of CdS gradually declined while the intensity of luminol increased. When the probe concentration was 100 ng mL^{-1}, the ratio of ECL intensity is large enough for the detection. Although the ratio increases with the increased concentration, the cathode ECL emission intensity is too small, leading to an increase of systemic error. Thus, 100 ng mL^{-1} of the probe was employed for the next experiments.

3.4. Analytical performance

Under the optimal conditions, the ratio ECL intensity of the immunosensor increased with the increasing concentration of CEA

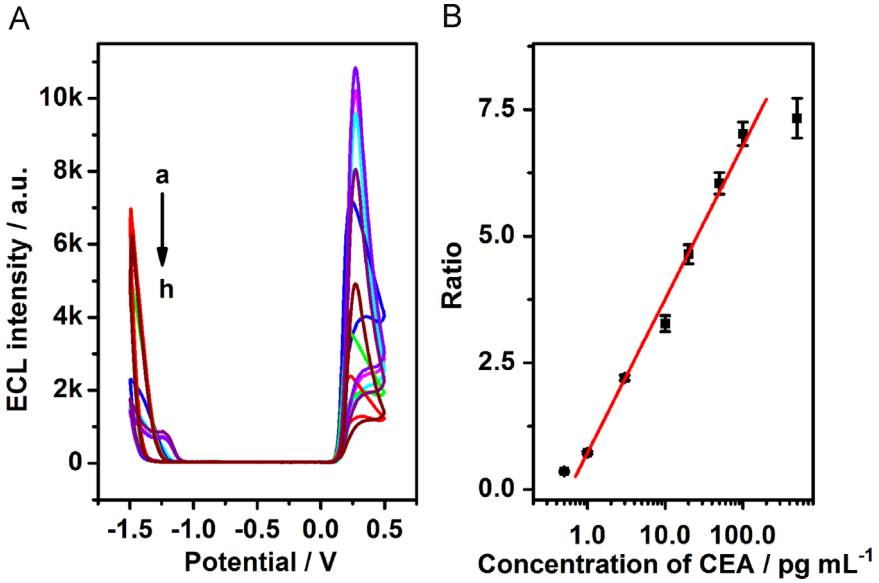

Fig. 4. (A) ECL response of the immunosensor in the detection of 0.5, 1.0, 3.0, 10, 20, 50, 100 and 500 pg mL^{-1} (from a to h) CEA in air-saturated pH 8.0 PBS buffer containing 0.1 M KNO_3 and 3.0 mM H_2O_2. Scan rate: 0.1 V s^{-1}. (B) Linear calibration between CEA concentration and the peak intensity ratio of anode to cathode ECL.

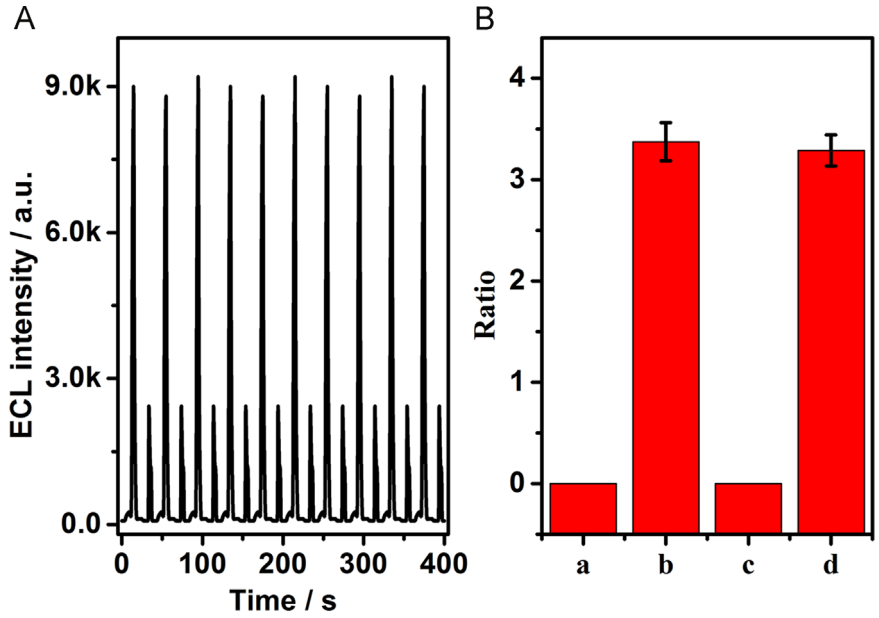

Fig. 5. (A) Continuous cyclic scans of the immunosensor with the ECL emissions of luminol (high) and CdS QDs (low) for 10 pg mL^{-1} CEA in air-saturated pH 8.0 PBS buffer containing 0.1 M KNO_3 and 3.0 mM H_2O_2. (B) Specificity of the biosensor in response to buffer (a), 10 pg mL^{-1} CEA (b), 100 pg mL^{-1} AFP (c), and 10 pg mL^{-1} CEA+100 pg mL^{-1} AFP (d). Scan rate: 0.1 V s^{-1}.

as a model analyte in the incubation solution (Fig. 4). The calibration plot showed a good linear relationship between the ratio of ECL intensity and the logarithm of the value of CEA concentration in the range from 1.0 pg mL^{-1} to 100 pg mL^{-1} with a correlation coefficient of 0.995. The limit of detection at a signal-to-noise ratio of 3 was 0.62 pg mL^{-1}, which is much lower than other ECL immunoassays (Cheng et al., 2012; Chen et al., 2013, 2014), and is comparable to 0.3 pg mL^{-1} of self-enhanced ECL immunosensor based on Pd nanowires (Wang et al., 2015). Also, this immunoassay method avoided the need of deoxygenation for ECL immunoassay, providing a good practicability.

3.5. Reproducibility and precision of immunosensor

The proposed biosensor showed stable ECL signal upon consecutive potential scans, indicating the feasibility for ECL detection. Both the intraassay and interassay precisions of the ECL immunosensor were examined five times in air-saturated pH 8.0 PBS buffer containing 0.1 M KNO_3 and 3.0 mM H_2O_2 at the presence of 10.0 pg mL^{-1} CEA. The relative standard deviations (RSD) were 2.5% and 5.6%, respectively, showing the good precision and acceptable fabrication reproducibility. Ten measurements of ECL emission upon continuous cyclic scans of the ECL immunosensor for 10.0 pg mL^{-1} CEA showed coincident signal with RSD of 0.74% (Fig. 5A), indicating acceptable reliability and stability of the detection signal. In addition, the sensor demonstrated the good selectivity against α-fetoprotein (AFP) (Fig. 5B). When the sensor was not in use, it was stored in air condition at room temperature and measured in pH 8.0 PBS buffer containing 0.1 M KNO_3 every few days. No obvious change in the ECL intensity was observed after storage for 4 weeks.

3.6. Application in detection of serum tumor marker

The analytical reliability and application potential of the proposed method was evaluated by comparing the assay results of clinical serum samples using the proposed ECL immunosensor. When the level of serum tumor marker was over the calibration range, serum samples were appropriately diluted with 0.02 M pH 7.4 PBS prior to assay. The CEA concentration in the samples was calculated to be 42.1 ± 0.4 pg mL^{-1} and 10.3 ± 0.2 pg mL^{-1} by standard addition method, which is consistent with the reference ECL analyzer (Elecsys 2010, Roche). When spiking with 10 and 50 pg mL^{-1} CEA standard solution, the average recoveries for three determinations were ranging from 95.0% ± 5.9% and 102.0% ± 9.6%, indicating the acceptable accuracy of the proposed method for the detection of CEA in clinical samples.

4. Conclusions

A novel sensitive dual-potential ECL ratiometric sensing strategy regulated by the electrocatalysis of highly-loaded Pd NCs@GO composite was constructed with CdS QDs and luminol as emitters. The probe was prepared by in-situ reduction of K_2PdCl_4 and luminol on graphene oxide with high simplicity and sensitivity. The probe not only highly loaded the Pd NCs and luminol to enhance the anode ECL of luminol but also competitively consumed the H_2O_2 coreactant to decline the cathode ECL of CdS QDs. Thus, the ratio ECL intensity between luminol and CdS QDs can be significantly enhanced at the proposed immunosensor via electrocatalysis of coreactant H_2O_2. On the construction of sandwich immunization, the ratio of anode to cathode ECL peak intensity has wide linear relationship with the concentrations of CEA. This method showed the low detection limit, excellent stability, good precision, acceptable reproducibility and reliability, providing an optional method for clinical diagnosis.

Acknowledgments

We gratefully acknowledge the National Natural Science Foundation of China (21375060, 21135002, 21121091) and Priority Development Areas of the National Research Foundation for the Doctoral Program of Higher Education of China (20130091130005).

References

Cao, W.D., Ferrance, J.P., Demas, J., Landers, J.P., 2006. J. Am. Chem. Soc. 128, 7572–7578.
Chen, H.F., Gao, Z.Q., Cui, Y.L., Chen, G.N., Tang, D.P., 2013. Biosens. Bioelectron. 44, 108–114.
Chen, L.C., Zeng, X.T., Si, P., Chen, Y.M., Chi, Y.W., Kim, D.H., Chen, G.N., 2014. Anal. Chem. 86, 4188–4195.
Cheng, Y., Huang, Y., Lei, J.P., Zhang, L., Ju, H.X., 2014. Anal. Chem. 86, 5158–5163.
Cheng, Y.F., Yuan, R., Chai, Y.Q., Niu, H., Cao, Y.L., Liu, H.J., Bai, L.J., Yuan, Y.L., 2012. Anal. Chim. Acta 745, 137–142.
Cui, H., Wang, W., Duan, C.F., Dong, Y.P., Guo, J.Z., 2007. Chemistry 13, 6975–6984.
Cui, H., Zou, G.Z., Lin, X.Q., 2003. Anal. Chem. 75, 324–331.
Deng, L., Du, Y., Xu, J.J., Chen, H.Y., 2014. Biosens. Bioelectron. 59, 58–63.
Deng, S.Y., Ju, H.X., 2013. Analyst 138, 43–61.
Dennany, L., Forster, R.J., Rusling, J.F., 2003. J. Am. Chem. Soc. 125, 5213–5218.
Ding, C.Q., Tian, Y., 2014. Biosens. Bioelectron. 65, 183–190.
Doeven, E.H., Zammit, E.M., Barbante, G.J., Francis, P.S., Barnett, N.W., Hogan, C.F., 2013. Chem. Sci. 4, 977–982.
Han, F.F., Jiang, H., Fang, D.J., Jiang, D.C., 2014. Anal. Chem. 86, 6896–6902.
He, L.L., Yang, X.H., Zhao, F., Wang, K.M., Wang, Q., Liu, J.B., Huang, J., Li, W.S., Yang, M., 2015. Anal. Chem. 87, 2459–2465.
He, Y., Cui, H., 2012. J. Mater. Chem. 22, 9086–9091.
Hu, B., Hu, L.L., Chen, M.L., Wang, J.H., 2013. Biosens. Bioelectron. 49, 499–505.
Jie, G.F., Liu, B., Pan, H.C., Zhu, J.J., Chen, H.Y., 2007. Anal. Chem. 79, 5574–5581.
Li, C.X., Lin, J., Guo, Y.S., Zhang, S.S., 2011. Chem. Commun. 47, 4442–4444.
Lin, D.J., Wu, J., Yan, F., Deng, S.Y., Ju, H.X., 2011. Anal. Chem. 83, 5214–5221.
Liu, J.F., Yan, J.L., Yang, X.R., Wang, E.K., 2003. Anal. Chem. 75, 3637–3642.
Liu, X., Zhang, Y.Y., Lei, J.P., Xue, Y.D., Cheng, L.X., Ju, H.X., 2010. Anal. Chem. 82, 7351–7356.
Nagaiah, T.C., Schäfer, D., Schuhmann, W., Dimcheva, N., 2013. Anal. Chem. 85, 7897–7903.
Noor, M.O., Krull, U.J., 2014. Anal. Chem. 86, 10331–10339.
Shin, I.S., Bae, S.W., Kim, H., Hong, J.I., 2010. Anal. Chem. 82, 8259–8265.
Sun, S.G., Sun, W., Mu, D.Z., Jiang, N., Peng, X.J., 2015. Chem. Commun. 51, 2529–2531.
Wang, H.J., Yuan, Y.L., Chai, Y.Q., Yuan, R., 2015. Biosens. Bioelectron. 68, 72–77.
Xu, S.J., Liu, Y., Wang, T.H., Li, J.H., 2011. Anal. Chem. 83, 3817–3823.
Yan, Y.H., Sun, J., Zhang, K., Zhu, H.J., Yu, H., Sun, M.T., Huang, D.J., Wang, S.H., 2015. Anal. Chem. 87, 2087–2093.
Yoon, C.H., Cho, J.H., Oh, H.I., Kim, M.J., Lee, C.W., Choi, J.W., Paek, S.H., 2003. Biosens. Bioelectron. 19, 289–296.
Zhang, H.R., Wu, M.S., Xu, J.J., Chen, H.Y., 2014. Anal. Chem. 86, 3834–3840.
Zhang, H.R., Xu, J.J., Chen, H.Y., 2013. Anal. Chem. 85, 5321–5325.
Zhang, Z.F., Cui, H., Lai, C.Z., Liu, L.J., 2005. Anal. Chem. 77, 3324–3329.
Zhao, M., Zhuo, Y., Chai, Y.Q., Yuan, R., 2015. Biomaterials 52, 476–483.
Zhao, W.W., Ma, Z.Y., Yan, D.Y., Xu, J.J., Chen, H.Y., 2012. Anal. Chem. 84, 10518–10521.